1st International Symposium on Laser Ultrasonics: Science, Technology and Applications
July 16-18 2008, Montreal, Canada

Laser Ultrasonics in Cylindrical Rods and Fibers

Damien SEGUR [1], Alexander SHUVALOV [1], Yongdong PAN [2], Clément ROSSIGNOL [1], Bertrand AUDOIN [1]

[1] Laboratoire de Mécanique Physique, UMR CNRS 8469, Université Bordeaux 1, 33405 Talence, France
[2]Institute of Acoustics, Tongji University, 200092, Shanghai, P. R. China

Abstract
Cylindrical parts are widely used in industry at very different scales from rotating axis for engines to carbon fibres used in composite materials. Consequently, an increasing demand exists for their non-destructive evaluation. The laser ultrasonics technique providing a non-contact generation and detection process is suited for the study of acoustic waves in cylindrical structures. In previous works, cylinders with a size in the millimetre range have been studied. In this paper, first results obtained on a tungsten micrometric fibre thanks to a pump-probe femtosecond laser technique are presented. Experiments are compared to a two-dimension model for acoustic waves generation and propagation in cylinders taking light penetration depth into account.
Keywords: Laser ultrasound, cylinders, Green function, optical penetration, fibres

1. Introduction

Having emerged in the 80s, the laser ultrasonics technique with its non-contact generation and detection feature overpasses the difficulties of coupling piezoelectric transducers with curved surfaces. To date, the authors [1] have been interested in acoustic generation for opaque cylinders where the acoustic source is located at the cylinder surface. In this work, assuming line focusing of the laser pulses, a two-dimension (2D) semi-analytic model for acoustic waves generation and propagation in a partly transparent isotropic cylinder is proposed. First, the radial displacement at any position on the free surface is derived, in a 2D Fourier domain, for an inner point source. The response to a volume source distribution along a radius is obtained as a convolution of the above Green function with the corresponding source distribution caused by optical absorption. Two inverse transforms are then applied to obtain the radial displacement at the cylinder surface. Second, picosecond ultrasonic experiments are performed on a tungsten micrometric fibre of 5 µm diameter and the results are compared with calculated waveforms.

2. Photoelastic generation in fibres

Let us consider a homogenous and isotropic cylinder of infinite length, radius a, and density ρ. Line focusing of a laser pulse at the cylinder surface along its z-axis is assumed. The temperature and elastic fields due to the laser line pulse along the z-axis direction are governed by the following coupled equations of thermoelasticity

$$\nabla.\left(\bar{\bar{\kappa}}:\nabla T\right)-\rho C_p\frac{\partial T}{\partial t}=Q-T_0\beta\nabla\cdot\frac{\partial u}{\partial t}$$
$$\rho\frac{\partial^2 u}{\partial t^2}-(\lambda+2\mu)\nabla\nabla.u+\mu\nabla\times\nabla u=-\beta\nabla T \qquad (1)$$

where $\bar{\bar{\kappa}}$ is the thermal conductivity tensor of the second order, T_0 the room temperature expressed in Kelvin, $\beta=3\lambda+2\mu$ the elastic modulus with λ and μ the Lame coefficients, and C_p the specific heat. The source term *Q* in the heat equation (1.1) is due to the laser optical pulse and corresponds to an optothermal energy conversion and is expressed in unit of a volume density power ([Wm^{-3}]). The second equation (1.2) stands for the equilibrium law where *u* is the displacement vector and $\beta=\beta/(\lambda+2\mu)$.

Thermal source $Q(r,\theta,t)$ expresses a volume distribution of optical sources in the cylinder due to optical absorption over a characteristic length α^{-1}, where α is the extinction coefficient. According to the symmetry of the problem, absorption phenomena lies essentially in the radial direction whereas orthoradial dependency is only due to the width of the line source included in the model by mean of the gauss function $g(\theta)=1/\left(2a\gamma\sqrt{\pi}\right)e^{-\theta^2/4\gamma^2}$ [m^{-1}], where γ is the angle corresponding to the line width. So, the thermal source *Q* can be written in the following form

$$Q(r,\theta,t)=\alpha E\delta(t)g(\theta)D(r),\ \text{where}\ D(r)=e^{-\beta r}\ \text{with}\ \begin{cases} r=a-r\ ,\ \text{if}\ \theta=0 \\ r=a+r\ ,\ \text{if}\ \theta=\pi \end{cases} \qquad (2)$$

The incoming laser line energy E_0 ([Jm^{-1}]) is partially reflected at the surface of the sample with the reflection coefficient *R*. Thus, the transmitted energy is given by $E=E_0(1-R)$.

Assuming that the evolution of the temperature field doesn't depend on the mechanical field *u* the coupling term can be neglected in equation (1.1) leading to a partly coupled thermoelasticity problem. In this work, interest is focused on materials with a very low thermal diffusivity and so heat conduction is neglected. First, solving Eq. (1.1) the temperature elevation field *T* is derived

$$\Delta T(r,\theta,t)=\frac{\alpha E}{\rho C_p}g(\theta)H(t)D(r) \qquad (3)$$

A temperature elevation field *T* is found out with a Heaviside time dependency $H(t)$ satisfying the assumption of no heat conduction. Then, thermal field being obtained one can solve the uncoupled mechanical problem

$$\nabla^2\varphi-\frac{1}{C_L{}^2}\frac{\partial^2\varphi}{\partial t^2}=\beta\nabla T$$
$$\nabla^2\psi-\frac{1}{C_T{}^2}\frac{\partial^2\psi}{\partial t^2}=0 \qquad (4)$$

where φ and ψ are the scalar and vector potentials, respectively, and C_L, C_T are the longitudinal, respectively shear wave velocities. Free boundary condition is considered

$$\begin{aligned}\sigma_{rr}(r=a)&=0\\ \sigma_{r\theta}(r=a)&=0\end{aligned} \tag{5}$$

3. Transformed displacement solution in term of potential Green function

In order to derive a solution to the above boundary value problem, let us derive the Green function $G(r|r_0)$, expressed in a potential form, for the interior problem of a dilatational line source located at the position $(r_0 < a, \theta = 0)$ inside the cylinder.

$$\begin{aligned}\nabla^2 g(r|r_0) - p^2 g(r|r_0) &= \beta_0 \frac{\delta(r-r_0)}{r_0}\\ \nabla^2 \psi(r|r_0) - s^2 \psi(r|r_0) &= 0\end{aligned} \tag{6}$$

with $p = \omega / C_L$ and $s = \omega / C_T$. Then the so-called Green function is explicitly given by

$$G(r|r_0) = \nabla g(r|r_0) + \nabla \times \psi(r|r_0) \tag{7}$$

where $g(r|r_0)$ and $\psi(r|r_0)$ are respectively the solution of (6.1) and (6.2).
Solution for (6.1) may be sought as a linear combination of the two independent solutions of the homogeneous Helmhotz equation[2]

$$g(r|r_0) = A_\nu J_\nu(pr) H(r_0 - r) + \left[B_\nu Y_\nu(pr) + C_\nu J_\nu(pr)\right] H(r - r_0),\ r_0 < a \tag{8}$$

where $H(r)$ corresponds to a radial Heaviside distribution. Solution of (6.2) yields another unknown constant D_ν

$$\psi(r|r_0) = D_\nu J_\nu(sr),\ r_0 < a \tag{9}$$

Thus four constants have to be found out injecting expressions of $g(r|r_0)$ and $\psi(r|r_0)$ into the two equations of boundary conditions. Consideration on continuity properties between the left hand side of equation (6.1) and the delta function in the right hand side gives two additional equations, which permit to determine the two other constants. Solving the corresponding linear system of equations allows one to derive the Green function for the radial displacement at a given position at the surface of the cylinder due to a dilatational line source located into the cylinder with the corresponding free boundary conditions.

$$G_r^V(a|r_0,\nu,\omega)=\frac{\pi\beta}{2a}J_\nu(pr_0)\left[Y_\nu(pa)\left(Y_a-\frac{E_\nu}{D_\nu}P_a\right)+\frac{2\nu^2}{\pi D_\nu}\left(1-\nu^2+\frac{s^2a^2}{2}\right)\right] \quad (10)$$

with $Y_a = paY'(pa)/Y(pa)$, $P_a = paJ'(pa)/J(pa)$, and where $D_\nu(\omega,\nu)=0$ corresponds to the dispersion equation, and

$$E_\nu=\left(\nu^2-\frac{s^2a^2}{2}\right)^2-\nu^2+\frac{s^2a^2}{2}(P_a+Y_a)+(1-\nu^2)P_aY_a \quad (11)$$

The radial displacement field is then derived thanks to a convolution between the radial component of the Green function $G_r^\nu(a|r_0)$, due to an inside dilatational line source, and the radial distribution of acoustic sources which is in our case related to the thermal field

$$U_r(a,\nu,\omega)=\int_0^{a-} G_r^V(a|r_0,\nu,\omega)T(r_0,\nu,\omega)r_0dr_0 \quad (12)$$

Finally, the radial displacement in the real space is obtained using a 2D inverse Fourier Transform. In order to avoid difficulties in numerical integration due to poles of the dispersion equation $D_\nu(\omega,\nu)=0$, Weaver [3] proposed to introduce a small imaginary part in the frequency variable $\omega^* = \omega - j\delta$ to move the poles off the real axis.

$$U_r(a,\theta,t)=\frac{e^{\delta t}}{2\pi}\int_{-\infty}^{+\infty}\sum_{\nu=-\infty}^{+\infty}U_r(a,\nu,\omega)e^{j(\nu\theta-\omega t)}d\omega \quad (13)$$

Noting that $U_r(a,\nu,\omega)$ is an even function of the variable ν, radial displacement can be rewritten as follows

$$U_r(a,\theta,t)=\frac{e^{\delta t}}{2\pi}\int_{-\infty}^{+\infty}\left\{\sum_{\nu=0}^{+\infty}U_r(a,\nu,\omega)\cos\nu\theta\right\}e^{-j\omega t}\,d\omega \quad (14)$$

4. Numerical and Experimental validation

A picosecond ultrasonics setup is used to perform experiments on a tungsten micrometric fibre with a diameter of 5 µm. Generation and detection points are spatially superimposed and shifted in time thanks to a delay line providing a time resolved technique [4]. Tungsten fibre is stretched at its bounds and is totally free of contact over a distance of one millimetre in order to prevent any perturbation of the cylindrical surface waves. The beam distortion detection (bdd) technique[5] is applied to measure reflectivity changes in the sample.

The wavelength of the pump beam is 400 nm whereas that of the probe beam is 800 nm, and the cross-correlation width of the two beams is measured as 1 µm. Experimental

result is compared to a numerical simulation obtained with the two-dimensional photoelastic model for fibres for a source width of 0.5 µm. Imaginary part of the frequency, used to remove poles from the real axis, is introduced with the numerical parameter $\delta = 0.02$. Material constants used for simulations are c_{11} = 522 GPa, c_{12} = 200 GPa, ρ = 19.3 g.cm^{-3}, and a small imaginary part is introduced in the stiffness coefficients $c_{ij}^{*} = c_{ij} + j\omega\eta$ with η = 0.05 GPa.s^{-1} to take the attenuation of acoustical waves into account. Reflection coefficient for tungsten is chosen to be R = 0.5.

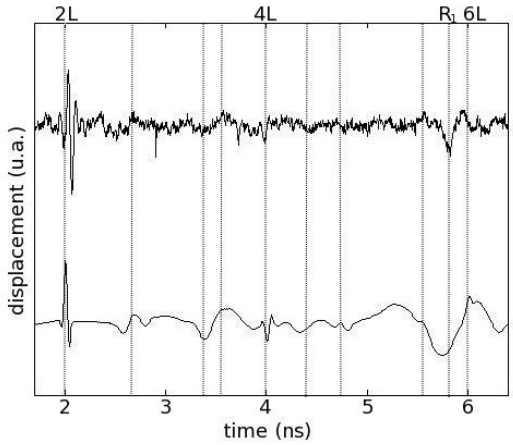

Figure 1. Comparison between experimental signal (top) and theoretical displacement (bottom) on a tungsten fibre of 5 µm diameter. The thermal background was removed from the experimental data

A quite good agreement is obtained (Fig.1) in term of time arrivals for the longitudinal waves 2*L*, 4*L* propagating back-and-forth through the fibre. Strong attenuation is observed for the 4*L* echo, which has travelled about 20 µm and encountered up to three successive reflections. As expected Rayleigh wave R_1 is clearly detected with a spread shape echo.

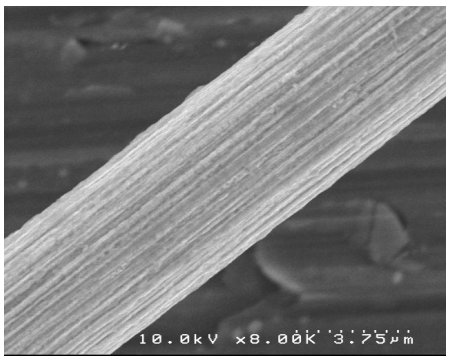

Figure 2. Photograph of a tungsten fiber with a micrometer diameter, captured by the Scanning Electron Microscopy

This comparison is a very first step in the understanding of acoustic waves propagation in such micrometric fibre. The mixture between strain and displacement in the measured signal provided by the bdd technique doesn't allow to clearly compare the shape of the echoes but only their time arrivals. Numerical simulation permits us to identify main arrivals as longitudinal reflections 2*L*, 4*L* and Rayleigh wave R_1. However, even if other

peaks are not clearly identified we can expect that some correspond to transverse waves or waves resulting of mode conversion. Then, it would be possible to obtain information on the stiffness coefficient c_{12}. One limitation concerns the building process of this kind of metallic fibres, which implies a quite bad surface quality of the fibre explaining the low Signal to Noise Ratio. Scanning Electron Microscopy technique provides an image (Fig.2) of the fibre surface and confirms the bad surface quality of the sample.

3. Conclusions

Time resolved picosecond ultrasonics technique is especially suited for the study of physical acoustics in micrometric or sub-micrometric structures. At these scales, photo-thermal mechanisms have to be considered for the waves generation process, taking the light penetration depth in the sample into account. A two-dimension photo-elastic model for generation and propagation of acoustic waves in cylindrical structures based on a radial displacement Green function has been proposed. Convolution theorem was then applied to obtain the response to a radial distribution of acoustic sources. Theoretical results are compared to a picosecond ultrasonics experiment on a tungsten micrometric fibre with a diameter of 5 µm. Good agreement is obtained in term of time arrivals and main echoes were identified including the diametrically sequences of longitudinal waves 2*L*, 4*L*, and the cylindrical Rayleigh wave R_1.

References

1. Y. Pan, C. Rossignol, B. Audoin, "Acoustic waves generated by a laser line pulse in a transversely isotropic cylinder", *Applied Physics Letters*, 82, pp 4379-4381, 2003.
2. G.N. Watson, *A treatise on the theory of Bessel functions*, Cambridge University Press, 1966.
3. R. Weaver, W. Sachse, K. Kim, "Transient elastic waves in a transversely isotropic plate", *J. Appl. Mech*. 63, pp 338-346, 1996.
4. C. Thomsen, J. Strait, Z. Vardeny, H.J. Maris, J. Tauc, J.J. Hauser, "Coherent phonon generation and detection by picosecond light pulses", *Phys. Rev. Lett*. 53(10), pp 989, 1984
5. N.V. Chigarev, C. Rossignol, B. Audoin, "Surface displacement measured by beam distorsion detection technique : application to picosecond ultrasonics", *Rev. Sci. Instrum*. 77(11), pp 114901, 2006.